

## Shape-controlled synthesis of novel precursor for fibrous Ni-Co alloy powders

ZHAN Jing<sup>1,2</sup>, ZHOU Di-fei<sup>1</sup>, ZHANG Chuan-fu<sup>1</sup>

1. School of Metallurgical Science and Engineering, Central South University, Changsha 410083, China;

2. State Key Laboratory for Powder Metallurgy, Central South University, Changsha 410083, China

Received 25 September 2010; accepted 28 February 2011

**Abstract:** A novel precursor of nickel-cobalt alloy powders with an appropriate Ni to Co molar ratio was prepared under selectively synthetic conditions. The composition and morphology of the precursor were characterized by X-ray diffractometry (XRD), scanning electron microscopy (SEM), Fourier transform infrared spectrometry (FT-IR) and energy dispersive spectrometry (EDS). The effects of pH value, reaction temperature, metal ion concentrations and surfactant on the morphology and the dispersion of precursor were investigated. The results show that the morphology of precursor depends on ammonia content in the precursor. A fibriform precursor is a complicated ammonia-containing nickel-cobalt oxalate. The uniform shape-controlled fibrous precursor is obtained under the following optimum conditions: ammonia as complex agent as well as pH adjuster, oxalate as coprecipitator, 50–65 °C of reaction temperature, 0.5–0.8 mol/L of total concentration of Ni<sup>2+</sup> and Co<sup>2+</sup>, PVP as dispersant, and pH 8.0–8.4.

**Key words:** fibrous precursor; Ni-Co alloy powder; shape-controlled synthesis; composition control; growth mechanism

### 1 Introduction

Bimetallic nanomaterials are paid to more attention because of their unique properties including considerable differences from their monometal counterparts[1]. Ni-Co alloys, important transition metal alloys, have high thermal conductivity, thermal stability, electrical conductivity, electrocatalytic activity and specific magnetic properties[2]. So they should be good high-temperature catalysts and specific magnetic materials, and can be applied in some high-temperature electrochemical devices, such as solid oxide fuel cells (SOFCs)[3], electromagnetic devices[4], microwave absorber and electromagnetic shielding material[5]. Especially, one-dimensional (1D) Ni-Co alloy nanoparticles are attracted by many scientists due to their distinctive geometry characteristics and novel chemical and physical properties such as shape anisotropy, magnetocrystalline anisotropy and exchange anisotropy. Many novel techniques have been employed to synthesize quasi 1D Ni-Co alloy materials including template[6], liquid-phase reduction[7], electrodeposition[8], microemulsion[9], sol-gel-thermal reduction[10], and magnetic-induced carbonyl decomposition[11].

However, the above synthetic methods require the use of hard templates, surfactant or external forces, which would result in difficulties in application of magnetic assemblies as nanodevices.

In the previous literatures, the pure solid solution of Ni-Co oxalates has been studied by many scientists[12]. Their researches aimed to prepare spherical nickel-cobalt alloy powders with accurate Ni to Co molar ratios at low pH values. In our previous research, fibrous nickel and copper powders were prepared by precipitation-thermal decomposition method[13–14]. It was found that once the particles with special morphology are formed, their basic characteristics, such as morphology, will be maintained. ZHANG et al[15] has reported that fibrous Ni-Co alloy powders without expected Ni to Co molar ratios were prepared by oxalate coprecipitation method. However, the problem between morphology and Ni to Co molar ratios cannot be solved. Moreover, the mechanism of fibre and composition of the precursor are not fully understood due to preferential precipitation of nickel oxalate or cobalt oxalate at different Ni to Co molar ratios. In this study, the morphology-controlled synthesis of the novel precursors with expected Ni to Co molar ratios and morphology was carried out and possible mechanism of formation of the one-dimensional

precursor particles was proposed.

## 2 Experimental

### 2.1 Synthesis process

Nickel chloride, cobalt chloride, oxalate, ammonium oxalate, polyvinylpyrrolidone (PVP 30), polyethylene glycol, polyacrylamide, sodium dodecylbenzenesulfonate (DBS), Gelafin, Tween 80, ammonia, ethanol and acetone were used as raw materials. All of the reagents were of analytical grade without further purification prior to use. Nickel chloride and cobalt chloride were mixed in a container according to different molar ratios of  $\text{Ni}^{2+}$  to  $\text{Co}^{2+}$ . Then the intimate mixture was injected into mixture-solvent medium containing oxalate or ammonium oxalate, organic solution and ammonia by a peristaltic pump under a certain temperature. Meanwhile, ammonia solution was added to adjust and stabilize the pH value. After agitating and aging, the coprecipitate was washed with distilled water followed by surfactant solution, ethanol, and acetone. Then the coprecipitate was filtered and dried in vacuum drier at 100–120 °C for more than 12 h. Finally, the precursor particles were obtained and subsequently heated at various temperatures in order to get nickel-cobalt alloy powders. The influencing factors on the morphology and dispersion of the precursor were also investigated by using initial molar ratio 4:1 of  $\text{Ni}^{2+}$  to  $\text{Co}^{2+}$ . Precursor particles with different molar ratios of Ni to Co were synthesized under the optimum operation conditions.

### 2.2 Characterization

The structure and composition of precursor particles were characterized by powder X-ray diffractometer (XRD), using  $\text{Cu K}\alpha$  radiation. The morphology, particle size and dispersion of the precursor were observed with JSM-5600LV electron scanning microscope (SEM). The infrared spectra (IR) were performed in the range of 4 000–400  $\text{cm}^{-1}$  by using Nexus470 spectrometer with the precursor particles dispersed in KBr at room temperature. Molar ratios  $\text{Ni}^{2+}$  to  $\text{Co}^{2+}$  were determined by chemical analysis and energy dispersive spectrometry (EDS).

## 3 Results and discussion

### 3.1 XRD patterns of precursors synthesized at different pH values

Fig.1 represents the X-ray diffraction patterns of the precursors prepared at different pH values. It can be found that XRD pattern of the precursor synthesized at pH=3.0 overlaps those of  $\alpha\text{-NiC}_2\text{O}_4\cdot 2\text{H}_2\text{O}$  and

$\beta\text{-CoC}_2\text{O}_4\cdot 2\text{H}_2\text{O}$  obtained at pH=3.0. The result confirmed the occurrence of Ni-Co oxalate solid solutions as reported by GAO et al[16]. The formula of the precursor prepared at pH=3.0 could be expressed as  $\text{Ni}_x\text{Co}_{1-x}\text{C}_2\text{O}_4\cdot 2\text{H}_2\text{O}$  ( $x=0-1$ ). However, the other three XRD patterns of the precursors obtained at  $\text{pH}\geq 6.0$  are obviously different from those of  $\text{Ni}_x\text{Co}_{1-x}\text{C}_2\text{O}_4\cdot 2\text{H}_2\text{O}$  and even no standard JCPDS card is consistent with them. Obviously, nickel and cobalt ions react with ammonia to form  $\text{Ni}_x\text{Co}_{1-x}(\text{NH}_3)_y$  ( $y=1-6$ ) and further react with oxalate to form a novel precursor due to an equilibrium between ammonia molecule and ammonium ions in coprecipitation process when  $\text{pH}\geq 6.0$ . This novel precursor is a complicated ammonia-containing nickel-cobalt oxalate instead of pure  $\text{Ni}_x\text{Co}_{1-x}\text{C}_2\text{O}_4\cdot 2\text{H}_2\text{O}$ .

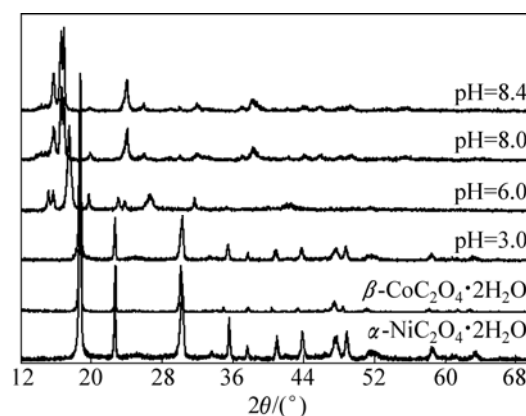
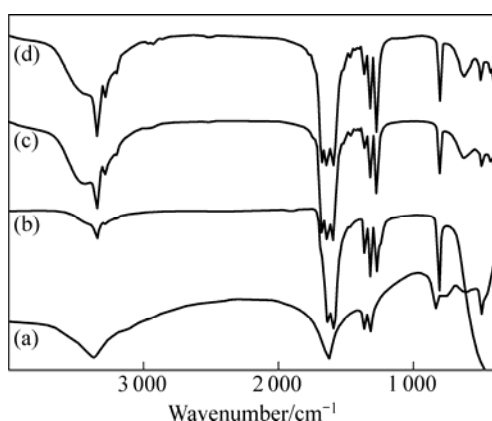


Fig.1 X-ray diffraction patterns of precursors prepared at different pH values

### 3.2 IR spectra of precursors prepared at different pH values

Fig.2 shows IR spectra of precursor particles prepared at various pH values. In Fig.2(a), several typical bands are observed. For instance, the strong band at 3 375  $\text{cm}^{-1}$  associates with stretching vibration of crystallization water; the strong band at 1 624  $\text{cm}^{-1}$  is due to H—O—H bending motion and C=O stretching vibration; the sharp doublet at 1 315 and 1 360  $\text{cm}^{-1}$  associate with C—O stretching vibration; the medium band at 824  $\text{cm}^{-1}$  is due to C—C stretching vibration; the band at 650–490  $\text{cm}^{-1}$  is due to M—O linkage. The above results are consistent with those reported in Ref.[17]. Fig.2(b) presents a displacement of the bands from 3 375  $\text{cm}^{-1}$  to 3 345  $\text{cm}^{-1}$ . The band at 1 632  $\text{cm}^{-1}$  contributes to the shift of band 1 624  $\text{cm}^{-1}$  and a new band at 1 587  $\text{cm}^{-1}$  is attributed to N—H bending vibration. The sharp doublet at 1 315 and 1 360  $\text{cm}^{-1}$  become sharp triplet at 1 268, 1 316 and 1 359  $\text{cm}^{-1}$  that are associated with C—O stretching vibration and C=O stretching vibration, respectively. Furthermore, there are band displacement at 824  $\text{cm}^{-1}$  to 815  $\text{cm}^{-1}$  and peak disappearance in the range of 650–490  $\text{cm}^{-1}$ , which may

be relative to the sample preparation process. The IR spectrum in Fig.2(c) is different from that in Fig.2(a). Band displacements from  $3\ 375\ \text{cm}^{-1}$  to  $3\ 348\ \text{cm}^{-1}$  and a new very weak band at  $3\ 284\ \text{cm}^{-1}$  are found, the later attributes to N—H stretching vibration. The band at  $1\ 624\ \text{cm}^{-1}$  split into three bands at  $1\ 677$ ,  $1\ 640$  and  $1\ 592\ \text{cm}^{-1}$ , of which the bands at  $1\ 677$  and  $1\ 592\ \text{cm}^{-1}$  could attribute to the bending vibration of N—H. In addition, there are three stretching vibrations of C—O or C=O ( $1\ 361$ ,  $1\ 317$ ,  $1\ 269\ \text{cm}^{-1}$ , respectively). In the range of  $824\text{--}490\ \text{cm}^{-1}$ , the above three bands positions are similar to those in Fig.2(a). Moreover, Fig.2(d) shows the similar IR spectrum pattern to Fig.2(c). Based on the above analysis, the results show that the precursor is  $\text{Ni}_x\text{Co}_{1-x}\text{C}_2\text{O}_4$  without ammonia when  $\text{pH}<6.0$ . When pH value increases, more  $\text{NH}_3$  begins to react with precursor, yielding the precursors of ammonium-containing nickel and cobalt oxalate rather than the pure precursors of nickel and cobalt oxalate.



**Fig.2** IR spectra of precursors at different pH values: (a)  $\text{pH}=3.0$ ; (b)  $\text{pH}=6.0$ ; (c)  $\text{pH}=8.0$ ; (d)  $\text{pH}=8.6$

IR spectrum analysis and  $\text{NH}_3$  emission during thermal decomposition further confirm that  $\text{NH}_3$  molecules exist in the precursor when  $\text{pH}\geq 6.0$ . In addition,  $\text{Ni}^{2+}$  and  $\text{Co}^{2+}$  reacted with  $\text{C}_2\text{O}_4^{2-}$  at chemical stoichiometry of 1:1. Therefore, it can be assumed that the chemical formula is  $\text{Ni}_x\text{Co}_{1-x}(\text{NH}_3)_y\text{C}_2\text{O}_4 \cdot z(\text{NH}_3) \cdot n\text{H}_2\text{O}$  ( $x=0\text{--}1$ ,  $y=1\text{--}6$ ,  $z=0\text{--}1$ ,  $n=1\text{--}2$ ), where  $x$ ,  $y$ ,  $z$  and  $n$  depend on experimental conditions.

### 3.3 Effects of technological conditions on morphology and particle size of precursor

#### 3.3.1 Effects of pH value

In this study, ammonia was used as pH value adjustor as well as complex agent in order to minimize the introduction of impurity ions in the solution. Fig.3 shows the SEM images of the precursors prepared at different pH values. It could be seen that pH value in solution plays an important role in the morphology and

size of precursor particles. When pH value is 5.0, the precursor particles display cubic-like morphology and the particles are aggregated (Fig.3(a)). When pH values range from 8.0 to 8.4, the precursor morphology is fibrous with satisfactory dispersion (Fig.3(b) and Fig.3(c)). However, when pH value is 8.8, the length of the fibrous precursor becomes short and the cluster of the fiber tends to be corroded (Fig.3 (d)). The precursor formation includes the formation and growth of crystal nuclear. Under low pH values, the precursor particles consist of  $\text{Ni}_x\text{Co}_{1-x}\text{C}_2\text{O}_4 \cdot 2\text{H}_2\text{O}$  and the concentration of free metal ions in solution is very high during nuclear formation and growth. A high concentration of free metal ions results in a relatively fast reaction rate, inhibiting the oriented growth of the precursor particles. With the increase of pH values, ammonia molecule coordinates with free metal ions to form complexes. The precursors are then converted to complicated Ni-Co oxalate particles after combination with  $\text{NH}_3$ . Thus, the formation complexes would greatly decrease the concentration of free  $\text{Co}^{2+}$  and  $\text{Ni}^{2+}$  in the solution. Such a low concentration of  $\text{Co}^{2+}$  and  $\text{Ni}^{2+}$  would reduce the reaction rate, which facilitates the oriented growth and assembly of the precursor particles. The higher the pH value is, the more the ammonia exists in the precursor. Therefore, it is reasonable to conclude that ammonia is morphology controller and pH value adjustor. However, at relatively higher pH values (higher than 8.8), more ammonia molecules could cause the dissolution of fibrous particles and lower ratio of axis to diameter.

#### 3.3.2 Effects of reaction temperature

As shown in Fig.4, temperature has significance effects on the morphology and particle size of the precursor. At relatively low temperatures, the aggregated precursors are obtained (Fig.4(a)). When the temperature elevates, the fine long fibrous particles are produced, as shown in Fig.4(b) and Fig.4(c). When reaction temperature is  $75\ ^\circ\text{C}$ , heat motion in the system strengthens, meaning much more opportunities for particles encountering. As a consequence, the length, width and thickness of particle increase (Fig.4(d)), and segregation of metal ions occurs. It is known that the crystal morphology eventually depends on the relatively competitive growth of the different crystal face orientation. The fast growing crystal face will certainly diminish and the slow growing crystal face may gradually emerge. The change of the physical and chemical condition may lead to the change of the unit structure patterns of the crystal growth and particle morphology. The temperature finally affects the nuclear formation and growth because the elevated temperature is beneficial for lowering the viscosity, increasing ion diffusion and promoting crystal growth. In this system, the oriented growth of axial crystal face into fibre was

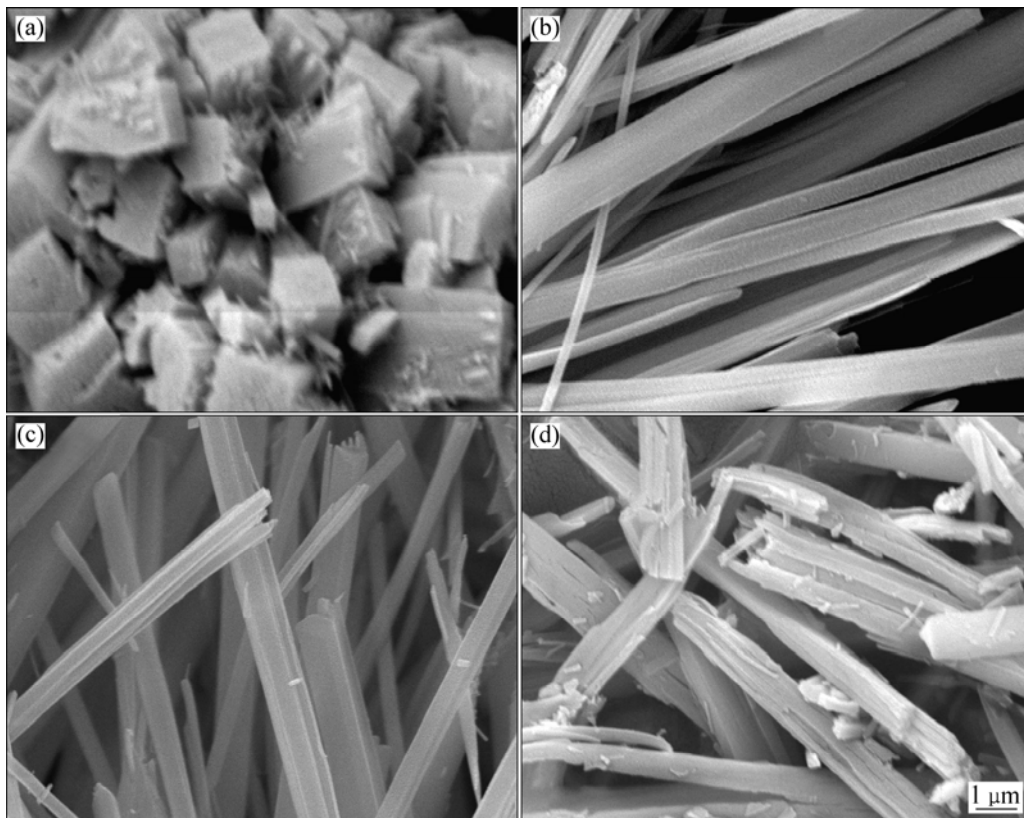


**Fig.3** SEM images of precursor particles synthesized at different pH values: (a) pH=5.0; (b) pH=8.0; (c) pH=8.4; (d) pH=8.8

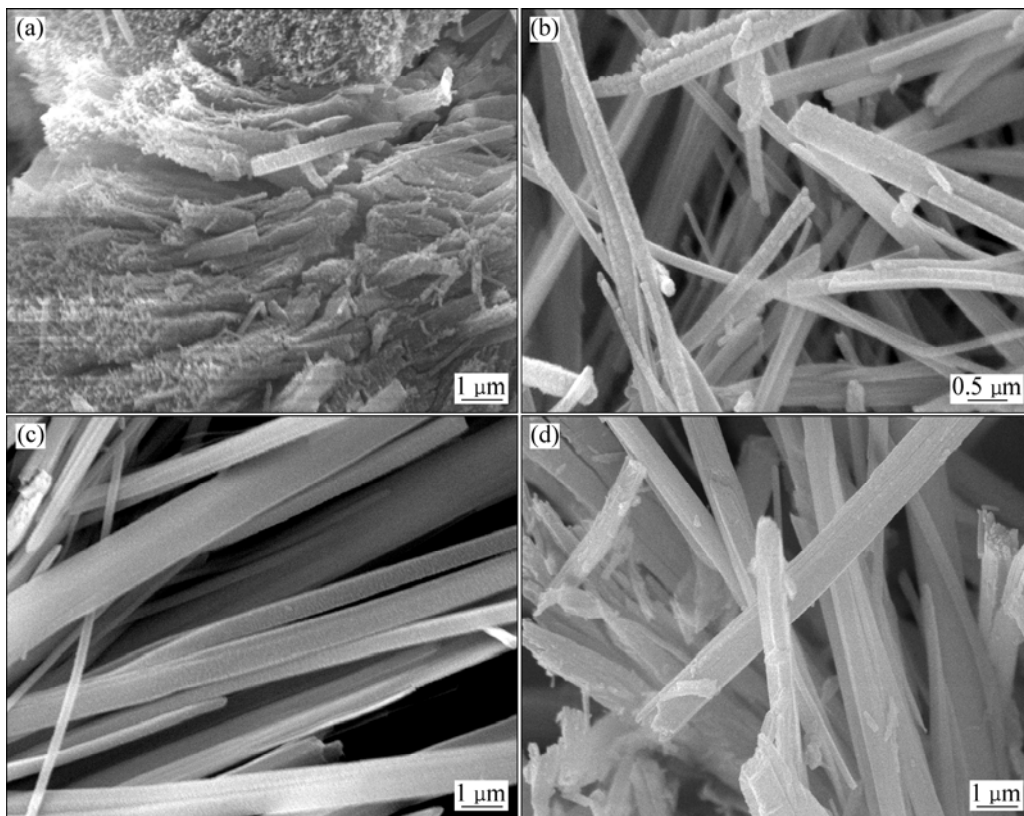


**Fig.4** SEM images of precursor particles obtained at different reaction temperatures at pH 8.2: (a) 40 °C; (b) 50 °C; (c) 60 °C; (d) 75 °C

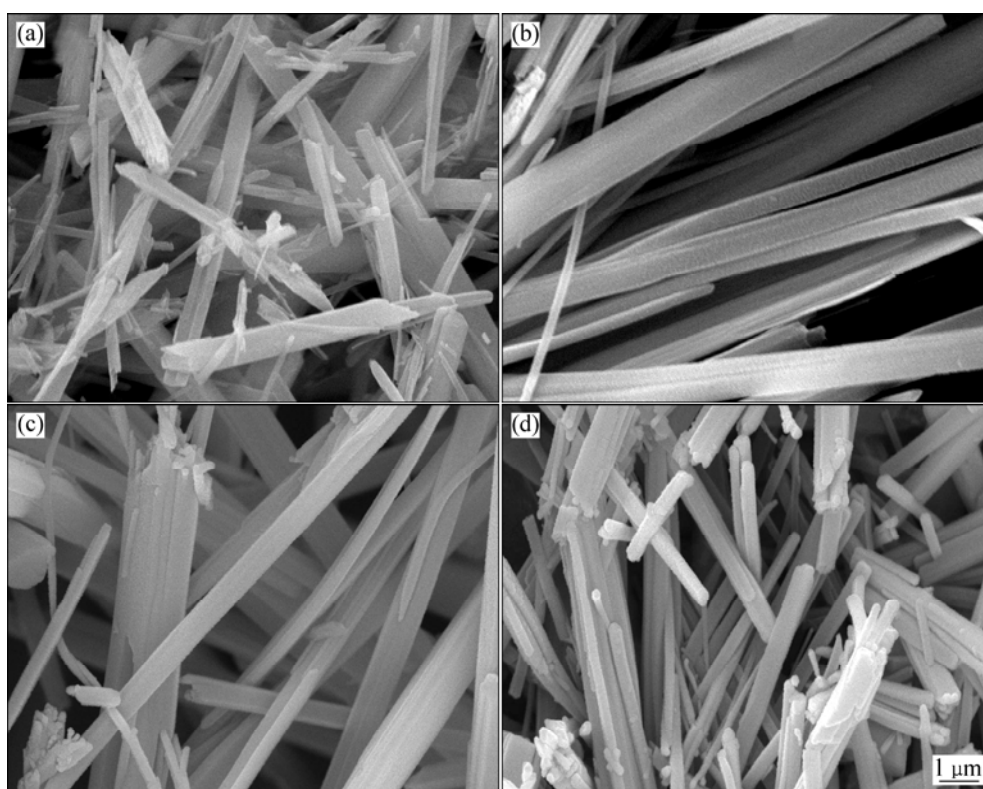


**Fig.5** SEM images of precursors obtained at different metal ion concentrations at pH 8.2: (a)  $c(\text{Ni}^{2+}+\text{Co}^{2+})=0.4$  mol/L; (b)  $c(\text{Ni}^{2+}+\text{Co}^{2+})=0.5$  mol/L; (c)  $c(\text{Ni}^{2+}+\text{Co}^{2+})=0.8$  mol/L; (d)  $c(\text{Ni}^{2+}+\text{Co}^{2+})=1.0$  mol/L

enhanced by the increased temperature.

### 3.3.3 Effects of metal ions concentration

Fig.5 displays SEM images of the precursor particles obtained at different metal ion concentration at pH 8.2. The morphological features of the precursor particles were related to the total concentration of nickel and cobalt ions. When the total concentration of metal ions is 0.4 mol/L, the precursor particles show aggregation of stick-like shape and the ratio of axis to diameter is relatively small (Fig.5(a)). However, the lengths of the particles increase with the increase of metal ion concentration, and the particles reveal crystal face in axial orientation. When the total concentration of nickel and cobalt ions is higher than 0.5 mol/L, the precursor particles display fibrous morphology with satisfactory dispersion, as shown in Figs.5(b) and (c). When the concentration of metal ions is 1.0 mol/L, the short-rod precursors are formed (Fig.5(d)). According to the classical cryallographic theory, particle formation includes two processes, nucleation and crystal growth. At lower metal ion concentration, the saturation degree in solution is relatively low, meaning slower nucleation rate. In this case, epitaxial and superficial growths of crystal predominate, which contributes to perfect crystallinity. On the contrary, exorbitant metal ion concentration will favor the explosion of nuclei and losing control of crystal growth. Therefore, proper initial metal ion concentration

is important for preparing the fine precursor particles with satisfactory morphology.

### 3.3.4 Effects of surfactant

Generally, addition of suitable surfactant is useful for improving the dispersion of the particles and producing small sized particles with specific morphology. The effect of the surfactant on the precursor was investigated and the results are shown in Fig.6. It is clear that the fibrous particles were obtained with addition of surfactant PVP 30. Moreover, Tween 80 can improve the dispersivity of precursor particles. However, this improvement was not observed for DBS, polyacrylamide, and polyethylene glycol; and the precursors were difficult to filter, resulting in the difficulties to be carried out experiment because of much foam. Gelafin had the reverse effects on hastening rod-like growth and aggregation of the precursor particles. Moreover, the optimum content of the surfactant PVP should be controlled in the range of 0.1%–0.5% (mass fraction).

## 3.4 Characterization and proposed growth mechanism of precursors

Table 1 represents the chemical contents of  $\text{Ni}^{2+}$  and  $\text{Co}^{2+}$  in the synthesized precursors. The precursors were formed under the conditions of pH=8.2,  $c(\text{Co}^{2+}+\text{Ni}^{2+})=0.6$  mol/L with varying molar ratios of  $\text{Ni}^{2+}$  to  $\text{Co}^{2+}$  in feed solution in terms of the required proportions,

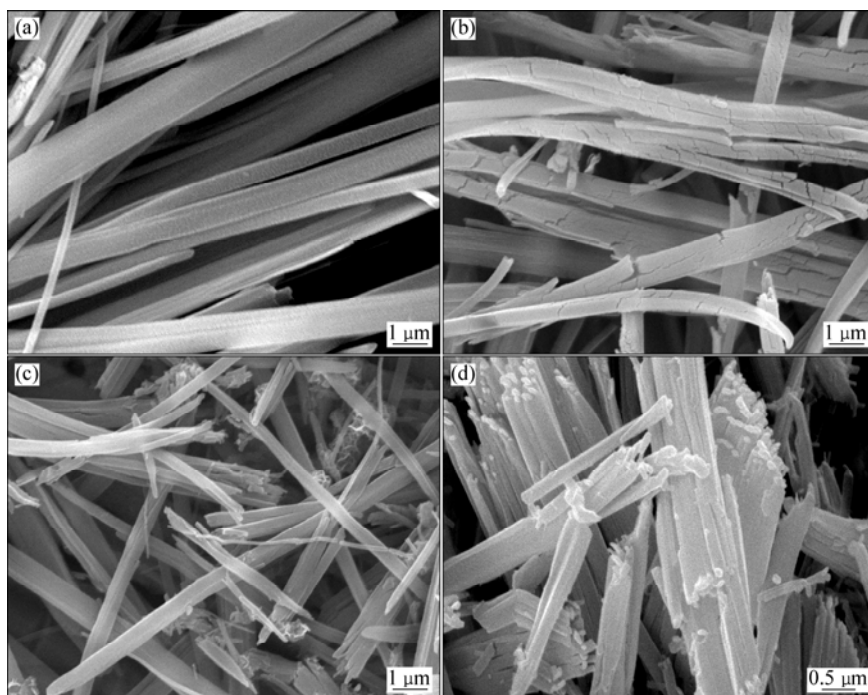


**Fig.6** SEM images of precursors obtained with different surfactants at pH 8.2: (a) PVP 30; (b) Tween 80; (c) DBS; (d) Gelafin

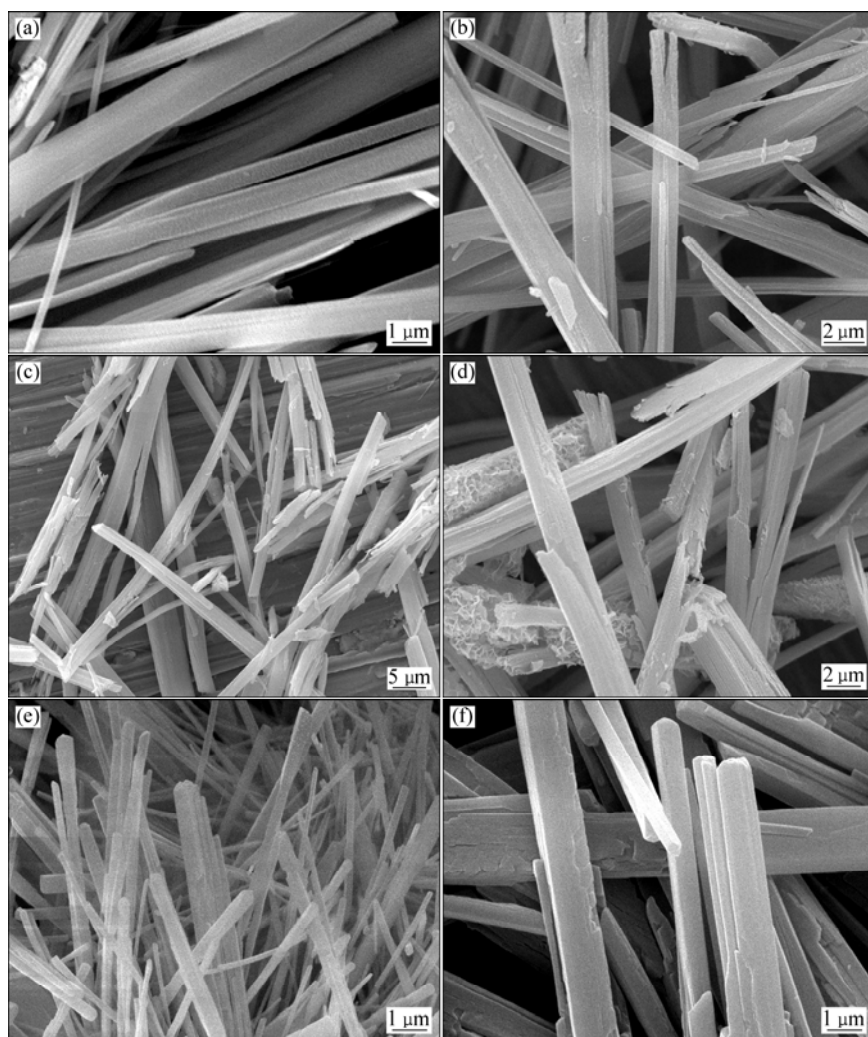


**Fig.7** SEM images of precursors with different molar ratios of  $\text{Ni}^{2+}$  to  $\text{Co}^{2+}$  prepared at pH 8.2,  $c(\text{Ni}^{2+}+\text{Co}^{2+})=0.6$  mol/L,  $t=60$  °C, 0.5% PVP: (a)  $n(\text{Ni}^{2+})/n(\text{Co}^{2+})=4:1$ ; (b)  $n(\text{Ni}^{2+})/n(\text{Co}^{2+})=7:3$ ; (c)  $n(\text{Ni}^{2+})/n(\text{Co}^{2+})=3:2$ ; (d)  $n(\text{Ni}^{2+})/n(\text{Co}^{2+})=1:1$ ; (e)  $n(\text{Ni}^{2+})/n(\text{Co}^{2+})=2:3$ ; (f)  $n(\text{Ni}^{2+})/n(\text{Co}^{2+})=3:7$

**Table 1** Chemical contents of Ni<sup>2+</sup> and Co<sup>2+</sup> in synthesized precursors

$n(\text{Ni}^{2+}):n(\text{Co}^{2+})$	4:1	7:3	3:2	1:1	2:3	3:7
$w(\text{Ni}^{2+})/\%$	28.01	23.90	19.98	15.76	13.50	9.38
$w(\text{Co}^{2+})/\%$	7.00	10.21	13.41	16.15	20.39	22.05

reaction temperature 60 °C and surfactant 0.5% (mass fraction). It is found that molar ratios of Ni<sup>2+</sup> to Co<sup>2+</sup> are fitted with the required ratios of the feed. The result confirms that shape-controlled synthesis of the fibrous precursors with expected molar ratios of Ni<sup>2+</sup> to Co<sup>2+</sup> could be obtained by coordination co-precipitation. SEM images of precursor particles prepared at different molar ratios of Ni<sup>2+</sup> to Co<sup>2+</sup> are shown in Fig.7.

The influence of experimental conditions on the morphology of nickel-cobalt oxalate is closely related to the structure of oxalate molecules crystal[18]. For the novel ammonia-containing precursor, the central metal atom was bonded by two C<sub>2</sub>O<sub>4</sub><sup>2-</sup> ions to form a planar molecule. Perpendicular to the molecular plane there are two coordinated H<sub>2</sub>O molecules by which crystal grain can grow in an elongate way along axial direction. The surface polar of Ni-Co oxalate molecules is different when the complex switches from H<sub>2</sub>O to NH<sub>3</sub> at different pH values by adding NH<sub>3</sub> in the solution. Thus, fibre-like precursor may be formed through [(NH<sub>3</sub>)M-OX-M(NH<sub>3</sub>)]<sup>2+</sup> growth units along the axial direction (OX represents C<sub>2</sub>O<sub>4</sub><sup>2-</sup>, M represents nickel or cobalt ion). Therefore, the formation ammonia-containing complex of oxalate nickel-cobalt was crucial to obtain fibriform precursor. The above complex was generated by coordination of ammonia and metal ions (such as nickel and cobalt ions) followed by the reaction with oxalate.

## 4 Conclusions

1) A novel precursor with required morphology and appreciate molar ratio of Ni to Co was prepared by coordinate coprecipitation technique. This precursor can be used for preparation of nickel-cobalt alloy particles. In order to obtain the required morphology, the synthetic conditions of fibrous precursors were chosen as follows: ammonia as complex agent and pH adjustor, oxalate as coprecipitated agent, pH 8.0–8.4, reaction temperature 50–65 °C, initial total nickel and cobalt salt concentrations 0.5–0.8 mol/L, addition of surfactant reagent (PVP), ethanol as rinsing agent and then 1 h immersion duration in ethanol. The precursor particles with different molar ratios of Ni to Co could be controlled accurately and reproducibly by varying the  $n(\text{NiCl}_2)/n(\text{CoCl}_2)$  values in the stock solution using mixing-solvent medium as coprecipitated medium.

2) At pH≤6.0, the formula of the precursor is

Ni<sub>x</sub>Co<sub>1-x</sub>C<sub>2</sub>O<sub>4</sub>·2H<sub>2</sub>O and the morphology is cubic-like aggregation. However, at pH≥8.0, the morphology of the precursor particles is fibrous and the formula of the precursor is presumed as Ni<sub>x</sub>Co<sub>1-x</sub>(NH<sub>3</sub>)<sub>y</sub>C<sub>2</sub>O<sub>4</sub>·zNH<sub>3</sub>·nH<sub>2</sub>O, where *x*, *y*, *z* and *n* represent mole numbers of the composition and their values depend on experimental conditions.

3) The crucial point for the formation of fibriform precursor is to yield ammonia-containing complex of oxalate nickel and cobalt. This complex is formed via the coordination of ammonia and metal ions followed by the reaction with oxalate.

## References

- [1] FERRANDO R, JELLINEK J, JOHNSTON R L. Nanoalloys: From theory to applications of alloy clusters and nanoparticles [J]. *Chem Rev*, 2008, 108(3): 845–910.
- [2] HU Ming-jun, LIN Bin, YU Shu-hong. Magnetic field-induced solvothermal synthesis of one-dimensional assemblies of Ni-Co alloy microstructures [J]. *Nano Res*, 2008, 1(4): 303–313.
- [3] ATKINSON A, BARNETT S, GORTE R T, IRVINE J T S, MCEVOY A J, MOGENSEN M, SINGHAL S C, VOHS J. Advance anodes for high-temperature fuel cells [J]. *Nat Mater*, 2004, 3(1): 17–27.
- [4] ZHANG Li, BAIN A J, ZHU Jian-gang, ABELMANN L, ONOUE T. Characterization of heat-assisted magnetic probe recording on CoNi/Pt multilayers [J]. *J Magn Magn Mater*, 2006, 305(1): 16–23.
- [5] ZHAN Jing, YUE Jian-feng, ZHANG Chuan-fu, FAN You-qi. Status preparation and application of quasi one-dimensional Ni-Co alloy material [J]. *Materials Review*, 2010, 24(5): 93–96. (in Chinese)
- [6] GHAREMANINEZHAD A, DOLATI A. A study on electrochemical growth behavior of the Co-Ni alloy nanowires in anodic aluminum oxide template [J]. *Journal of Alloys and Compounds*, 2009, 480(2): 275–278.
- [7] LIU Qi-ying, GUO Xiao-hui, WANG Tie-jun, LI Yong, SHEN Wei-jie. Synthesis of CoNi nanowire by heterogeneous nucleation in polyol [J]. *Mater Lett*, 2010, 64(11): 1271–1274.
- [8] CÉCILE G, PIERRRE L, WAROT-FONROSE B. Electrochemical synthesis of cobalt nickel nanowires in an ethanol-water bath [J]. *Mater Lett*, 2008, 62(14): 2106–2108.
- [9] ZHANG Dong-en, NI Xiao-min, ZHANG Xiao-jun, ZHENG Hua-gui. Synthesis and characterization of Ni-Co needle-like alloys in water-in-oil microemulsion [J]. *J Magn Magn Mater*, 2006, 302(2): 290–293.
- [10] SHEN Xiang-qian, CAO Kai, ZHOU Jian-xin. Preparation of ferromagnetic binary alloy fine fibers by organic gel-thermal reduction process[J]. *Transaction of Nonferrous Metals Society of China*, 2006, 16(5): 1003–1008.
- [11] XIE Wei, CHENG Hai-feng, CHU Zeng-yong, CHEN Chao-hui. Development on preparation of magnetic metallic fiber absorbers [J]. *Journal of Materials Engineering*, 2008(3): 72–76. (in Chinese)
- [12] ZHANG Chuan-fu, WU Lin-lin, LI Chang-jun, WU Jian-hui. Preparation of fiber precursor of Ni-Co alloy powder [J]. *The Chinese Journal of Nonferrous Metals*, 2002, 12(1): 182–186. (in Chinese)
- [13] ZHANG Chuan-fu, WU Jian-hui, ZHAN Jing, LI Chang-jun, DAI Xi. Precursor synthesis of fibrillar nanocrystalline nickel powder [J]. *Nonferrous Metals*, 2003, 55(3): 25–29. (in Chinese)
- [14] FAN You-qi, ZHANG Chuan-fu, WU Jian-hui, ZHAN Jing, YANG Ping. Composition and morphology of complicated copper oxalate

- powder [J]. Transactions of Nonferrous Metals Society of China, 2010, 20(1): 165–170.
- [15] ZHANG Chuan-fu, WU Lin-lin, LI Chang-jun, WU Jian-hui. Preparation of fiber precursor of Ni-Co alloy powder [J]. The Chinese Journal of Nonferrous Metals, 2002, 12(1): 182–186. (in Chinese)
- [16] GAO X, CHEN D, DOLLIMORE D, SKRZYPCZAK-JANKUN E, BURCKEL P. Identification of solid solutions of coprecipitated Ni-Co oxalates using XRD, TG and SEM techniques [J]. Thermochemica Acta, 1993, 220: 75–89.
- [17] GARCIA-CLAVEL M E, MARTINEZ-LOPE M J, CASAIS-ALVAREZ T. Thermal study of  $\text{NiC}_2\text{O}_4 \cdot \text{H}_2\text{O}$  obtained by solid state reaction at room temperature and normal pressure [J]. Thermochemica Acta, 1987, 118: 123–134.
- [18] JONGEN N, BOWEN P, LEMAITRE J, VALMALETTE J C, HOFMANN H. Precipitation of self-organized copper oxalate polycrystalline particles in the presence of hydroxypropyl-methylcellulose (HPMC): control of morphology [J]. J Colloid Interface Sci, 2000, 226(1): 189–198.

## 形貌控制法合成一种新型的纤维状镍钴合金粉末前驱体

湛 菁<sup>1,2</sup>, 周涤非<sup>1</sup>, 张传福<sup>1</sup>

1. 中南大学 冶金科学与工程学院, 长沙 410083;
2. 中南大学 粉末冶金国家重点实验室, 长沙 410083

**摘 要:** 通过选择性控制合成条件, 制备一种新型的纤维状镍钴合金粉末前驱体。该前驱体中镍、钴摩尔配比精确。采用 X-射线衍射仪(XRD)、扫描电镜(SEM)、红外光谱(FT-IR)和能谱(EDS)研究前驱体粉末的成分与形貌; 考察溶液 pH 值、反应温度、金属离子浓度和表面活性剂对前驱体粉末的形貌和分散性的影响。结果表明: 前驱体的形貌取决于前驱体中氨的含量, 这种纤维状前驱体为一种复杂的含氨草酸镍钴复盐。形貌控制合成纤维状镍钴合金粉末前驱体的最佳条件为: 氨作为配位剂和 pH 值调节剂, 草酸为沉淀剂, 反应温度为 50~65 °C, 镍、钴离子总浓度为 0.5~0.8 mol/L, PVP 为分散剂, 溶液 pH 值控制在 8.0~8.4。

**关键词:** 纤维状前驱体; 镍钴合金粉; 形貌控制合成; 成分控制; 生长机理

(Edited by YANG Hua)